Preparation, characterization, and in vitro cytogenotoxic evaluation of a novel dimenhydrinate-β-cyclodextrin inclusion complex

Lamija Hindija[1]*, Jasmina Hadžiabdić[1]*, Anja Haverić[2], Ognjenka Rahić[1], Maida Hadžić Omanović[2], Lejla Čaluk Klačar[2], Irma Durmišević[2], Amina Tucak Smajić[1], Merima Šahinović[1], and Edina Vranić[1]

[1]Department of Pharmaceutical Technology, Faculty of Pharmacy, University of Sarajevo, Sarajevo, Bosnia and Herzegovina.

[2]Laboratory for Cytogenetics and Genotoxicology, Institute for Genetic Engineering and Biotechnology, University of Sarajevo, Sarajevo, Bosnia and Herzegovina.

*Corresponding authors: Lamija Hindija; Email: lamija.hindija@ffsa.unsa.ba; Jasmina Hadžiabdić; Email: jasmina.hadziabdic@ffsa.unsa.ba.

ABSTRACT

Dimenhydrinate (DMH), used to alleviate motion sickness symptoms such as nausea, vomiting, dizziness, and vertigo, encounters limitations in oral pharmaceutical formulations due to its poor water solubility and bitter taste. Our research hypothesized that inclusion complexation with β-cyclodextrin (β-CD) might address these drawbacks while ensuring that the newly formed complexes exhibit no cytotoxic or genotoxic effects on peripheral blood mononuclear cells (PBMCs). Inclusion complexes were prepared using the kneading method and the solvent evaporation method. The phase solubility analysis, attenuated total reflectance-fourier transform infrared spectroscopy (ATR-FTIR), and differential scanning calorimetry (DSC) were conducted to evaluate the complexation efficacy and stability constant of the new binary systems. The results demonstrated that both methods provided complete and efficient complexation. Cytogenotoxic analysis, including the 3-[4,5-dimethylthiazol-2-yl]-2,5-diphenyl tetrazolium bromide (MTT) assay, alkaline comet assay, and cytokinesis-block micronucleus cytome (CBMN-cyt) assay, was conducted to assess the cytogenotoxic potential of DMH-β-CD inclusion complexes, a topic previously unexamined. No cytotoxic or genotoxic effects were observed within the concentration range of 36.36 to 109.09 ng/mL. Cell viability of treated PBMCs exceeded 85% for all tested concentrations. No significant increases in DNA strand breaks were observed at any dose, and tail intensity of all complexes remained lower or up to 2.2% higher than the negative control. Parameters indicating genotoxic effects, as well as cytotoxic and cytostatic potential in the CBMN-cyt assay, did not significantly differ from untreated controls. These results suggest that inclusion complexation with β-CD might be a safe and promising solution to overcome the limitations of poor solubility and unpleasant taste of DMH, potentially providing opportunities for new and improved oral pharmaceutical dosage forms.

Keywords: Dimenhydrinate; β-cyclodextrin; phase solubility; FTIR; DSC; MTT assay; alkaline comet assay; CBMN-cyt.

INTRODUCTION

Almost a third of the world's population is highly prone to motion-caused nausea, vomiting, dizziness and vertigo. Motion sickness is induced by a sensory mismatch, a syndrome triggered by a contradiction between the sensory system of balance and vision [1] and it can significantly affect one's general health, performance and quality of life [2]. Dimenhydrinate (DMH) is an over-the-counter drug used for the prevention and treatment of these conditions [3]. Comprising two drugs, diphenhydramine (2-diphenylmethoxy-N,N-dimethylethylamine) and 8-chlorotheophylline (Figure 1), DMH engages a dual action. Diphenhydramine acts as the primary antiemetic, alleviating neural excitation through H1 receptor antagonism, while 8-chlorotheophylline counteracts diphenhydramine's sedative effects by blocking adenosine A2 receptors [4]. DMH is a white, odorless and bitter crystalline powder, classified as a slightly soluble drug with log P of 3.65 and molar mass of 470 g mol^{-1}. It belongs to class II of Biopharmaceutical Classification System (BCS) as a drug with low solubility and high permeability [5,6]. A peak plasma concentration (C_{max}) of 72.6 ng mL^{-1} is reached after oral administration of 50 mg [7].

The growing interest in designing new drug-delivery systems stems from the necessity to enhance existing therapies for individual patient needs. To expedite the process and minimize costs associated with new drug development, attention has shifted towards improving pharmaceutical formulations using familiar active pharmaceutical ingredients (APIs) with established safety profiles. Cyclodextrins (CDs) have emerged as effective auxiliary substances for modifying undesirable physicochemical properties of known APIs, facilitating the development of advanced drug-delivery systems [8].

CDs, cyclic oligosaccharides with a hydrophilic outer surface and a lipophilic inner cavity, consist of 6 - 12 glucose units linked cyclically by α-1,4 glycosidic bond. They form inclusion complexes by incorporating drug molecules ("guests") into the internal CD cavity ("hosts"). Established non-covalent bond improves guest molecules' physicochemical properties

4

without necessitating chemical changes that are important for their therapeutic profiles. Inclusive complexation provides solubility increment of poorly soluble drugs (BCS class II or IV), ultimately increasing dissolution rate, bioavailability and release profile, and might as well mask guest's unpleasant taste or smell. [8,9].

CD complexation enhances the oral bioavailability of poorly water-soluble drugs with high lipophilicity (log P > 2.5), administered at low doses (< 100 mg) with DMH being an optimal candidate for complexation [10], due to its low solubility (3 mg mL^{-1}) [5], high lipophilicity (3.65) [3] and low dosage (25 or 50 mg in oral formulations) [11]. Its suitability is attributed to meeting specific requirements, including a skeleton with more than five C and N atoms, only two condensed rings, melting point below 250 °C, hydrophilic functional groups, and less than five condensed rings [10].

β-cyclodextrin (β-CD) is readily available and the size of its internal cavity (~ 6.5 Å) is optimal for the inclusion complex formation with a wide range of drugs [12]. Its molar mass is 1135 g mol^{-1} [13] and its aqueous solubility is 18.5 mg mL^{-1} [14] due to the cyclic structure, high crystal lattice energy and formation of intramolecular hydrogen bonds [15] (Figure 2). Given the substantial impact of API's solubility on its effectiveness, absorption, dissolution rate, and bioavailability, enhancing the solubility of poorly soluble drugs is crucial for ensuring their adequate therapeutic efficacy upon oral administration. The formation of inclusion complexes emerges as a potential solution to overcome limited solubility issues [16,17].

This work was built upon the hypothesis that inclusion complexation with β-CD will not only improve DMH solubility but also mask its bitter taste [18] and that newly formed complexes will exhibit neither cytotoxic nor genotoxic effects on peripheral blood mononuclear cells (PBMCs).

We aimed to comprehensively examine the inclusion complexes of DMH and β-CD that can be used in new, improved oral pharmaceutical formulations. Increased solubility of DMH,

and subsequently its bioavailability, provided by the complexation with β-CD should ensure a reduction of the dose required for therapeutic effect and, thus, reduction of toxic and other side effects [9]. Phase solubility study was conducted to evaluate the effects of β-CD on DMH aqueous solubility in liquid state, while the characterization of formed inclusion complexes in solid state was carried out by Attenuated Total Reflectance-Fourier transform infrared spectroscopy (ATR-FTIR) and differential scanning calorimetry (DSC). Furthermore, to ensure the safety of implementing these inclusion complexes in oral pharmaceutical formulations and to dismiss the possibility of cytotoxic or genotoxic effects after their administration, additional cytogenotoxic analyses were performed *in vitro*. Pure DMH, β-CD and their inclusion complexes prepared by two different methods were tested in concentration range from 36.36 to 109.09 ng mL^{-1}. DMH reaches a plasma concentration of 72.6 ng mL^{-1} when it is applied in a dose of 50 mg [7], and 14.5 ng mL^{-1} when it is applied in a dose of 25 mg [19], while the concentration of 600 ng mL^{-1} is considered toxic [20]. Data about the cytotoxicity and genotoxicity of DMH and inclusion complexes with β-CD are lacking therefore, these newly formed complexes were investigated by implementing 3-[4,5-dimethylthiazol-2-yl]-2,5 diphenyl tetrazolium bromide (MTT) assay, alkaline comet assay and cytokinesis block micronucleus cytome (CBMN cyt) assay in human lymphocyte cultures.

MATERIALS AND METHODS

Chemicals

Dimenhydrinate (2-benzhydryloxy-N,N-dimethylethanamine;8-chloro-1,3-dimethyl-7H-purine-2,6-dione, series 87081, code 3000402) was obtained as a donation from Bosnalijek, d.d. (Bosnia and Herzegovina). Kleptose® (β-CD; batch E1220) was generously gifted from Roquette (France). Ethanol 96% (V/V) was purchased from Kefo® d.o.o. (Bosnia and Herzegovina), chloroform and hydrochloric acid, 37% pro analisi (p. a.) were purchased from Merck KgaA (Germany). Histopaque® - 1077 (density 1.077 g/mol) , a sterile, endotoxin-

tested solution of polysucrose and sodium ditriazoate, was obtained from Sigma - Aldrich®
(St. Louis, MO, US) as well as Cytochalasin B (≥98%), cell-permeable mycotoxin that
inhibits cytoplasmic division by blocking the formation of contractile microfilaments, and
Roswell Park Memorial Institute Medium (RPMI - 1640) with L-glutamine and sodium
bicarbonate. PB-MAX™ Karyotyping Medium, a fully supplemented, RPMI-based medium
containing fetal bovine serum, L-glutamine, and phytohemagglutinin was purchased from
GIBCO Invitrogen (Carlsbad, CA). MTT (3-[4,5-dimethylthiazol-2-yl]-2,5 diphenyl
tetrazolium bromide, 98%) reagent, dimethyl sulfoxide (DMSO, ≥99.7%),
ethylenediaminetetraacetic acid disodium salt (Na_2EDTA, 99-101%), sodium hydroxide
(NaOH, 99+%), low melting point agarose (LMPA), normal melting point agarose (NMPA),
potassium chloride (KCl, 99.8-100.5%), glacial acetic acid 99.8%, 7-imino-N,N-
dimethylphenothiazin-3-amine;hydrochloride (Giemsa), 4',6-diamidinio-2-phenylidole
(DAPI 1 mg mL^{-1}) were purchased from Sigma - Aldrich® (St. Louis, MO, US).

Phase solubility studies

Phase solubility studies were performed according to Higuchi and Connors' method [21].
The excess amount of DMH was added into β-CD aqueous solutions with various
concentrations (8.81 - 22.03 mmol L^{-1}). Sample solutions were prepared as described by
Hindija et al [22]. Solutions with concentrations of 15.86 mmol L^{-1}, 17.62 mmol L^{-1} and
22.03 mmol L^{-1} were mixed at 50 °C for 24 h due to limited aqueous solution of a β-CD.
After the equilibrium was reached, the aliquots were filtered through a 0.2 μm pore size
membrane filter (Cellulose acetate filter, Sartorius, Germany), diluted with 0.1 M
hydrochloric acid and DMH concentration was determined spectrophotometrically at 277 nm
(Shimadzu UV spectrophotometer-1601, Kyoto, Japan). Each measurement was run in
triplicate.

Phase solubility studies, where the change of drug solubility corresponds to CD concentration, were conducted to assess the binding characteristics of the drug and CD and to determine the values of stability constant (K_s), complexation efficacy (CE) and utility number (U_{CD}). When a linear relationship between the solubility of the drug and the concentration of CD is obtained, K_s (M^{-1}) and CE can be determined from the equations (1) and (2):

$$K_s = \frac{Slope}{S_o\ (1 - Slope)} \quad (1) \qquad\qquad CE = K_s S_o = \frac{Slope}{1 - Slope} \quad (2)$$

where S_o is the molar solubility (mol L^{-1}) of the drug (its aqueous solubility in the absence of β-CD) and Slope denotes the slope of the straight line (slope of the phase solubility profile). CE values can be used to calculate the drug: cyclodextrin (D : CD) ratio, according to equation (3) [23]:

$$D : CD = 1 : \left(1 + \frac{1}{CE}\right) \quad (3)$$

Utility number, $U_{CD,}$ is expressed as:

$$U_{CD} = \frac{K\,S_o}{1 + K\,S_o}\frac{CD_t}{D_t} = \frac{K\,S_o}{1 + K\,S_o}\frac{m_{CD}}{m_D}\frac{MW_D}{MW_{CD}} \quad (4)$$

where m_D and m_{CD} are the drug dose and workable amount of CD in mg, respectively, while MW_D and MW_{CD} stand for molecular weights of D and CD [22].

Preparation of inclusion complexes

Preparation of inclusion complex by kneading method

Physical mixture preparation preceded inclusion complex formation. DMH and β-CD were accurately weighted (Analytical scale Mettler Toledo AT Balance, AT 400, Switzerland) in an appropriate 1 : 1 molar ratio, determined after the phase solubility analysis. Pure substances were separately pulverized. Powders were added in equivalent molar ratios,

carefully blended in a glass mortar into a homogeneous mixture and sieved through sieve No. 20 (Erweka VT/VS, Germany). Prepared physical mixture was triturated in a glass mortar with a small amount of water-ethanol solution (1 : 1 w/w) to obtain a homogeneous paste. The thick slurry was kneaded for 1 h and appropriate quantity of water-ethanol solution was intermittently added to maintain a suitable consistency. The newly formed compound was rinsed several times with a small amount of chloroform [24]. The paste was dried in a vacuum oven (Binder VD-23, Slovenia) for 6 h at 75 °C ± 0.5 °C, at pressure of 6 ± 2 mbar. The dried mixture was pulverized into a fine powder and sieved through sieve No. 20 (Erweka VT/VS, Germany).

Preparation of inclusion complex by solvent evaporation method

DMH and β-CD were accurately weighed in 1 : 1 molar ratio and separately dissolved in a sufficient quantity of ethanol according to their solubility using ultrasonic bath (Bandelin Sonorex, Germany). When clear solutions were obtained, solutions of DMH and β-CD were combined and the resultant solution was stirred on a magnetic stirrer (Witeg, WiseStir MSH-20D, Germany) for 30 minutes at 400 rpm (30 × g) and 25 °C. The solvent was evaporated under vacuum at 40 °C in a rotary vacuum evaporator (Ingos RVO 200A, Czech Republic). The obtained mixture was dried in a vacuum oven (Binder VD-23, Slovenia) for 6 h at 75 °C ± 0.5 °C, at pressure of 6 ± 2 mbar. The dried mixture was pulverized into a fine powder and sieved through sieve No. 20 (Erweka VT/VS, Germany).

Attenuated Total Reflectance-Fourier Transform Infrared Spectroscopy

ATR-FTIR spectra of pure DMH, β-CD, their physical mixture and inclusion complex prepared by kneading and solvent evaporation method were recorded using Cary 360 FTIR (ATR) spectrophotometer, Agilent, USA. Samples were placed on a disc and the plunger was pressed tightly to hold the sample. The spectra were collected from 32 scans, recorded in 4000 - 650 cm^{-1} scanning range at 4 cm^{-1} resolution.

Differential scanning calorimetry

DSC analysis of DMH, β-CD, their physical mixture and inclusion complexes prepared by kneading and solvent evaporation method was performed using a differential scanning calorimeter DSC 204F1 Phoenix (NETZCH - Geratebau GmbH, Selb, Germany). Samples of 3 - 10 mg were accurately weighed, placed in 25 μL aluminum pans, and heated at a scanning rate of 10 °C min^{-1} over the temperature range from 50 °C to 400 °C. An empty pan was used as a reference standard. The measurements were carried out under dry nitrogen at a flow rate of 20 mL min^{-1}. Each run was repeated in triplicate.

Cytotoxic and genotoxic studies

Analyses of the cytotoxic and genotoxic potential of DMH, β-CD and their inclusion complexes prepared by kneading and solvent evaporation method and their impact *in vitro* were assessed in human lymphocyte cultures, obtained from healthy male, 37 years old, non-smoking volunteer. Blood was collected by venipuncture into heparinized vacutainers (BD Vacutainer Systems, Plymouth, UK), stored at room temperature, protected from light and processed within 2 h. PBMCs were isolated by density gradient centrifugation (400 × g, 30 minutes) with separation medium (Histopaque® - 1077) [25]. After isolation, PBMCs were stained with Trypan blue and counted using a hemocytometer.

3-[4,5-dimethylthiazol-2-yl]-2,5 diphenyl tetrazolium bromide assay

MTT assay is regarded as a sensitive and reliable colorimetric assay to quantify cellular viability, proliferation and activation. It is based on the ability of mitochondrial nicotinamide adenine dinucleotide phosphate (NADPH)-dependent cellular oxidoreductase enzymes present in viable cells to reduce soluble tetrazolium salt (3-[4,5-dimethylthiazol-2-yl]-2,5 diphenyl tetrazolium bromide) to insoluble, colored formazan compounds [26].

DMH was administered in a concentration range from 36 ng mL^{-1} to 109 ng mL^{-1}. β-CD was applied in concentration from 0 - 1000 ng mL^{-1} while its highest concentration in the inclusion complex was 263.45 ng mL^{-1}. 5-fluorouracil (5-FU) at concentration of 1 mg mL^{-1}

was used as a positive control [27–30]. Untreated cells were set as negative control and their viability is expected to remain unchanged, while the medium without cells was considered as a blank to confirm the efficacy of the test procedure itself [31].

The MTT assay was conducted in triplicate in the 96-well plate, with two technical replicates. The seeding density was 6.25×10^3 cells per each well. Cells were incubated at 37 °C in an atmosphere of 5% CO_2 and then treated with DMH and β-CD solutions.

After the 72 h of incubation, the reagent MTT was added to samples for 3 h at 37 °C. DMSO was added to solubilize the formazan crystals followed by a further incubation for 30 and 60 minutes at 37 °C. The optical density was measured at 570 nm using multiplate reader Multi-Scan FC (Thermo Fisher Scientific, US). The cell viability was determined according to equation (5):

$$\text{Cell viability (\%)} = \frac{A_{(treatment)}}{A_{(negative\ control)}} \cdot 100 \quad (5)$$

Alkaline comet assay

Comet assay is a sensitive technique for measuring deoxyribonucleic acid (DNA) damage at the level of the individual eukaryotic cell. Comet assay is based upon the fact that denatured cleaved DNA fragments, or damaged DNA, migrate out of the cell at a different rate during electrophoresis than undamaged DNA [32]. Damaged DNA creates a "comet tail", while the undamaged DNA remains within the cell membrane creating the "comet head". Comet assay is most commonly run under alkaline conditions to detect single and double-stranded DNA breaks [33].

PBMCs were isolated as previously described and then cultivated in PB-MAX™ Karyotyping medium and incubated for 24 h at 37 °C. After incubation, PBMCs were treated with DMH, β-CD, their inclusion complexes prepared by kneading and solvent evaporation methods at the same concentrations as for the MTT assay. Positive and negative controls were also set up equally. Treated cells were incubated at 37 °C for 3 h, and then centrifuged

at 800 rpm (120 × g) for 5 minutes. The supernatant was removed and the cells were subsequently resuspended.

In a tube containing 120 μL of 0.7% LMPA, 80 μL of sample was added for each tested concentration, and controls. Prepared samples were applied to slides precoated with a 1% NMPA and covered with coverslips. After gel polymerization, coverslips were removed and slides were immersed into lysis buffer overnight at 4 °C. Afterward, slides were washed with distilled water and placed into electrophoresis tank with an electrophoresis solution (200 mM Na_2EDTA, 10 M NaOH and distilled water, pH > 13), for 20 minutes, followed by 20 minutes of electrophoresis (1 V/cm). After electrophoresis, slides were gently rinsed in the following sequences: phosphate buffer saline (PBS) for 5 minutes, 70% (V/V) ethanol for 5 minutes and finally 96% (V/V) ethanol for 15 minutes.

Prior to the fluorescent microscope analysis (U-MNU2; Olympus BX51, Tokyo, Japan), slides were rehydrated and stained with DAPI (1 μg mL^{-1}). DNA damage in treated cells was evaluated using Comet Assay IV software (Instem LSS Ltd., Staffordshire, UK), by measuring tail intensity (TI%), a percent of DNA in tail of comets. For each concentration, as well as for positive and negative controls, at least 200 comets were analyzed. MIRCA protocol was used to report the results [34].

Cytokinesis block micronucleus cytome assay

CBMN cyt assay is a widely used assay to evaluate cytotoxicity, DNA damage, and cytostatic effects in different tissue types [35].

In vitro analysis of the cytotoxic and genotoxic potential of DMH and its inclusion complexes with β-CD prepared by kneading and solvent evaporation method was performed applying CBMN cyt assay in PBMCs. DNA damage events were scored specifically in once-divided binucleated (BN) cells and included micronuclei (MNi), a biomarker of chromosome breakage and/or whole chromosome loss, nucleoplasmic bridges (NPBs), a biomarker of DNA misrepair and/or telomere end-fusions, and nuclear buds (NBUDs), a biomarker of

12

elimination of amplified DNA and/or DNA repair complexes [36]. Cytostatic and cytotoxic effects were examined by the calculation of the nuclear division index (NDI) and nuclear division cytotoxicity index (NDCI) based on the proportion of mono-, bi- and multinucleated cells and necrotic and/or apoptotic cell ratios, respectively.

Whole blood, 400 μL per each treatment, was cultured in PB-MAX™ Karyotyping Medium for 72 h at 37 °C. Treatments were added to the cultures in the 25th h of cultivation to the final concentrations of DMH 72.73, 90.91 and 109.09 ng mL^{-1} in samples with pure DMH and with complexes. Untreated cultures were set up as negative controls. Cytochalasin B was added to the final concentration of 4.5 μg mL^{-1}, to block cytokinesis.

After the cultivation period, cultures were centrifuged for 10 minutes at 1000 rpm (188 × g) and subjected to hypotonic treatment with 0.56% KCl and centrifuged immediately after the hypotonic addition. Hypotonic treatment was followed by three fixations in ice-cold glacial acetic acid + ethanol (1 + 3) fresh fixative. Fixed lymphocyte solution was dropped on coded microscope slides. Air-dried slides were stained in 5% Giemsa for 7 minutes. Frequencies of MNi, NPBs and NBUDs were observed under the 400X magnification in at least 2000 BN cells for each treatment. Frequencies of mononuclear, binuclear, trinuclear, and quadrinuclear cells, as well as apoptotic and necrotic cells, were scored in the total number of at least 500 cells. All genotoxicity and cytotoxicity parameters were recognized according to the criteria given by Fenech [37,38].

Statistical analysis

Statistical analyses were conducted on the results of cytotoxic and genotoxic studies to identify any significant differences among the tested samples of DMH, β-CD, their inclusion complexes at concentrations of 36.36, 54.55, 72.73, 90.91 and 109.09 ng mL^{-1}, as well as positive and negative controls. The Shapiro-Wilk test was used to assess the normality of distribution for MTT assay parameters, revealing that the data follows a normal distribution. One-way analysis of variance (ANOVA) was implemented, followed by a post-hoc Tukey-

Kramer test. Normality of distribution of Comet assay parameters was examined using Kolmogorov-Smirnov test. Afterward, the Kruskal-Wallis nonparametric test was conducted, succeeded by Dunn's multiple comparison test. Normality of distribution for CBMN cyt genotoxicity parameters was assessed by Shapiro-Wilk test. Accordingly, Kruskal-Wallis nonparametric test followed by Conover post-hoc analysis was applied to test significance of differences between tested concentrations of DMH and its inclusion complexes with β-CD in concentrations of 72.73, 90.91 and 109.09 ng mL^{-1} and controls (negative and positive). To estimate the relationship between NDI and NDCI values in different concentrations simple linear regression was used. Statistical analyses were performed using Microsoft Excel 2016, GraphPad Prism 8.4.3. (GraphPad Software Inc.; San Diego, CA, USA) and MedCalc®v.18.9 (MedCalc bvba, Ostend, Belgium) and values were considered significantly different for $p < 0.05$.

RESULTS

Phase solubility studies

Results of conducted phase solubility analysis and determined parameters were shown in Figure 3, Table 1 and Table 2.

Attenuated Total Reflectance-Fourier Transform Infrared Spectroscopy

The ATR-FTIR spectra of binary systems (physical mixture, inclusion complexes prepared by kneading method and solvent evaporation method) were compared to those of the pure substances (DMH and β-CD) (Figure 4). It was investigated whether characteristic bands of the pure substances changed, which will indicate the existence of a complex as a new compound with different spectroscopic bands.

Comparison between the intensity of FTIR signals of pure DMH and its physical mixture, inclusion complexes prepared by kneading method and solvent evaporation method with β-CD were given in Table 3. Comparison between the intensity of FTIR signals of pure β-CD and its binary systems with DMH (physical mixture and inclusion complexes prepared by

14

kneading method and solvent evaporation method) were given in Table 4. Tables included calculated chemical shift changes ($|\Delta\delta|$) in the samples and transmittance expressed in %.

Differential scanning calorimetry

DSC analysis was carried out to examine the behavior of individual components, their physical mixture and inclusion complexes prepared by the kneading method and the solvent evaporation method during heating (Figure 5), such as crystallization, phase transformation, dehydration and decomposition.

3-[4,5-dimethylthiazol-2-yl]-2,5 diphenyl tetrazolium bromide assay

Stock solution of DMH and its inclusion complexes with β-CD prepared by kneading and solvent evaporation method in RPMI-1640 Medium and PB-MAX™ Karyotyping Medium were diluted and applied as treatments with five increasing concentrations, together with blank, positive and negative control. Results of cell viability in human PBMCs in the presence of pure DMH, pure β-CD and their inclusion complexes were shown in Figure 6. ANOVA analysis showed that there was a significant difference between administered treatments ($p < 0.05$). Post-hoc Tukey Kramer test showed there were no statistically significant differences between negative control and treatments with pure DMH. However, statistically significant differences were perceived for pure β-CD and inclusion complexes prepared by kneading method and solvent evaporation method. Negative control and all of the treatments were significantly different from positive control. Another analysis was run to establish which concentration of pure β-CD and inclusion complexes prepared by kneading and solvent evaporation method differ from negative control. A statistically significant difference between treatments and negative control was recorded only for the highest concentrations. For the lower concentration of treatments, there were no significant differences compared to the negative control.

Alkaline comet assay

Genotoxic effects of DMH, pure β-CD and their inclusion complexes prepared by kneading and solvent evaporation method were expressed as a percent of DNA in the tail of comets (TI-tail intensity), based on analysis of 205 comets for each concentration (Table 5).

Tail intensity was not significantly increased for any of the treatments in comparison with negative control (untreated cells). All treatments, as well as negative control, were significantly different from positive control (cells treated with 5-FU).

Comet images recorded for treatments of PBMCs with pure DMH, pure β-CD and their inclusion complexes prepared by kneading and solvent evaporation method at highest concentrations (for DMH and inclusion complexes 109.09 ng mL^{-1} and for pure β-CD 1000 ng mL^{-1}) are shown in Table 6.

Cytokinesis block micronucleus cytome assay

Results of CBMN cyt assay are presented in Table 7 and they showed a significant decrease (p = 0.002) of total MNi frequency in all treatments with inclusion complex prepared by solvent evaporation method and in treatment with pure DMH in the lowest concentration (72.73 ng mL^{-1}) compared to negative control. Certainly, for those treatments, the same results were obtained for the frequency of BN cells with micronuclei (p = 0.001). The frequency of NBUDs was significantly decreased in all treatments compared to positive control (F = 2.725; p = 0.015) while for frequency of NPBs and values of NDI and NDCI, the significant differences were not found.

DISCUSSION

The complexes were prepared by two different methods, kneading method and solvent evaporation method, both involving adequate organic solvents to ensure that all or at least a small part of the components are brought into the solution so that a secondary bond can be formed between the molecules which provide the formation of inclusion complexes with proper stability [39]. Kneading method is simple, efficient and provides a good yield of

formed inclusion complexes. It is convenient for the preparation of complexes with poorly soluble drugs because of drug dispersion during complex formation [40,41]. The solvent evaporation method is simple, economical and suitable for large-scale preparation of complexes [42]. To the best of our knowledge, this topic has not yet been investigated in any published studies. Complexes of DMH were prepared either with different hydrophilic derivates of β-CD [43] or with different methods [44,45]. However, the effects on the viability of human lymphocytes have not been explored yet.

A-type phase solubility isotherms are characteristic of water-soluble complexes. Phase solubility diagram in this study revealed an A_L type isotherm, indicating that the solubility of DMH linearly increased with increasing β-CD concentration (Figure 3). Slope, defined as the change of y-axis (concentration of DMH) for a one unit increase in x-axis (β-CD concentration), indicates the steepness of a regression line. If one molecule of drug forms a complex with one molecule of CD, the slope of a straight line is less than unity and the value of K_S can be calculated by applying Equation (1). That was the case here, the slope value was 0.7751 implying the linear DMH solubility enhancement in β-CD solution and formation of a 1 : 1 complex.

Optimal K_s values range from 100 - 5000 M^{-1}. Lower values imply very labile complexes with premature drug release and insignificant solubility improvement. Higher values imply very stable complexes with incomplete or obstructed drug release from the CD cavity [10]. CE determination, reliant on the phase-solubility profile slope, is a suitable parameter for evaluating the solubilizing potential of CDs and less variable indicator than Ks, influenced by the intercept and intrinsic solubility affected by formulation excipients. In our case, the values of K_s (171.10 M^{-1}) and CE (3.45) pointed formation of a stable complex with expected appropriate drug release and satisfying solubility improvement. Solubility enhancement factor values (Table 1) indicate that a notable solubility enhancement is attained in solutions with a β-CD concentration of 15.86 mmol L^{-1} and above.

Values of the dimensionless number, $U_{CD} \geq 1$ implicate adequate solubilization provided by the complexation by CDs. Values ≥ 1 indicates sufficient solubilization through CD complexation, while values below 1 signify incomplete solubilization [46]. The calculated U_{CD} value for 1% (w/w) β-CD concentration was insufficient for complete solubilization of 25 mg DMH mL^{-1} water. The calculated U_{CD} value for 1% (w/w) β-CD concentration was < 1 implying that it was insufficient for complete solubilization of 25 mg DMH mL^{-1} water. A concentration of 1.8% (w/w) would be required to adequately provide dissolution of 25 mg DMH mL^{-1} of water. In that case, U_{CD} value is 1.156. D : CD ratio, based on the CE values equaled 1 : 1.29 and confirmed the formation of a 1 : 1 inclusion complex.

In ATR-FTIR spectrum of pure DMH (Figure 4A), characteristic peak at 3059.6 cm^{-1} corresponded to its amino groups. A sharp, stretched peak at 1644.3 cm^{-1} was for C=O stretching, at 1112.9 cm^{-1} was the peak for C=C stretching of the aromatic rings and at 749.3 cm^{-1} was the peak for C-Cl stretching of the carbonyl chloride [5,47].

In the spectrum of pure β-CD (Figure 4B), a peak at 3317.3 cm^{-1}, represents the vibration of symmetrical and asymmetrical stretching of primary hydroxyl (-OH) groups on C6 atoms of glucose molecules, located on the narrower side of the β-CD ring and another peak that appeared at 2926.0 cm^{-1} showed the vibration of -CH and -CH$_2$ groups. The peak at 1645.60 cm^{-1} may be attributed to residual H-O-H molecules and -OH groups in the glucose moieties of β-CD. The displayed peak at 1153.6 cm^{-1} originated from an ether-like bond between cyclically linked glucose molecules of β-CD. A distinct, sharp peak at 1019.4 cm^{-1} was assigned to the C-O-C stretching vibrations [6,48,49].

In a physical mixture of DMH and β-CD (Figure 4C) peak of DMH originating from its amino groups was overlapped by the peak of β-CD ascribed to the -OH stretching vibrations. The peaks ascribed to -CH$_2$ and -CH, H-O-H and C-O-C bending vibrations of β-CD and the peak corresponding to C=O and C-Cl stretching vibrations of DMH were shifted as shown in Table 3. The peak at 751.1 cm^{-1} is a result of the deformation vibrations outside of the

18

plane (δ) and flexion of -CH bonds of the aromatic core. Peaks characteristic for pure substances that were still observed in the spectrum of physical mixture imply that the DMH molecule was not entirely embedded into the β-CD cavity.

The spectra of inclusion complexes of DMH and β-CD prepared by the kneading method (Figure 4D) and solvent evaporation method (Figure 4E) differ from the spectra of pure substances (Figures 4A and 4B) and their physical mixture (Figure 4C). The shifts and intensity changes of the peak of pure β-CD ascribed to the -OH, -CH and -CH$_2$ stretching vibrations were shown in Table 4. The peak of DMH ascribed to the amino group was not identified, while peaks associated with the C=C stretching of the aromatic rings, C=O and C-Cl stretching in DMH molecule had different wavelengths and intensities in the spectra of inclusion complexes (Table 3). Embedding of DMH molecule into the central cavity of β-CD can also be confirmed due to significant changes in the intensity and wavelength of the peak characteristic for H-O-H stretching vibrations pointing that water molecules were shifted out of the cavity by DMH molecules. Insertion of the benzene part ring into the electron-rich cavity of β-CD increased the density of the electron cloud, thus leading to the frequency changes. Different frequencies of peaks in the inclusion complexes compared to the pure molecules appeared due to the changes in the microenvironment caused by hydrogen bonds formation and Van der Waals forces occurrence. The penetration of the guest molecule that occurs when the inclusion complex is formed caused consequent structural rearrangement of the H-bonded scheme in the host's inner cavity, which can be proved by changes of specific peaks' shapes, positions and intensities with respect to the pure compounds and physical mixture [50].

DSC is one of the best tools to confirm complex formation by the disappearance of the characteristic endothermic peaks of the drug in the thermogram of formed inclusion complex [51]. When guest molecules are embedded in the CD cavity, their melting, boiling, or

sublimation point generally could shift to a different temperature or disappear within the temperature range where CD was decomposed [52].

Figure 5A presents the DSC thermogram of pure DMH. Sharp, prominent endothermic peak at 106.2 °C appeared at its melting point [53]. Decomposition of the drug occurred at temperatures above 250 °C [54]. DSC thermogram of pure β-CD (Figure 5B) showed an endothermic peak at 110.8 °C attributed to the liberation of crystal water from β-CD. A small peak observed at 235 °C may be due to the glass transition and finally, the degradation of β-CD was at 322.5 °C [55,56].

DSC curve of the physical mixture of DMH and β-CD (Figure 5C) showed endothermic peaks at 102.1 °C (melting point of DMH), 120.8 °C (dehydration of β-CD) and 247.4 °C (decomposition of DMH). The slight changes that were observed in the melting endotherm for DMH (decreased temperature and intensity) indicated that there was a weak interaction between DMH and β-CD in a simple physical mixture.

In the thermograms of inclusion complexes of DMH and β-CD prepared by kneading method (Figure 5D) and solvent evaporation method (Figure 5E), the peak characteristic for the melting point of DMH disappeared which indicated successful inclusion complexation of DMH into the central cavity of β-CD. The formation of an inclusion complex was suggested not only by the absence of the melting endotherm of DMH, but also, by the reduction of the dehydration curve in the inclusion complex prepared by kneading method (Figure 5D) compared to the physical mixture (from 120.8 °C to 107.4 °C). That implies the displacement of water molecules by DMH. The endothermic peak that corresponds to the dehydration of β-CD was not identified in the inclusion complex prepared by the solvent evaporation method (Figure 5E). The complete disappearance of DMH's endothermal peak can be assumed as proof of interactions with β-CD. This can be considered as an indication of drug amorphization and/or inclusion complex formation. The disappearance of a sharp

endothermic peak in the range of the decomposition of the pure DMH is due to its encapsulation in the host's inner cavity.

Obtained results of MTT assay led to the conclusion that applied treatments with DMH, β-CD and their inclusion complexes did not reduce cell viability because there were no significant differences compared to the negative control. Only the treatments with the highest concentrations of pure β-CD (1000 ng mL^{-1}) and inclusion complexes prepared by both methods (DMH's concentration 109.09 ng mL^{-1}), which are considerably higher than therapeutic concentrations (72.6 ng mL^{-1}), were significantly different from negative control. Recorded cell viability for these concentrations was 90.3% for β-CD, 91.1% for inclusion complex prepared by kneading method and 85.8% for inclusion complex prepared by solvent evaporation method. Cell viability of negative control was considered to be 100% because those cells were untreated. Recorded cell viability for positive control was 64.8%, which significantly differ from negative control and all treatments ($p < 0.05$). According to Gokarn et al, DMH may slightly affect the viability of HEK293 cells [57]. Previous similar studies reported that β-CD does not affect cell viability on HeLa cells [58], LO2 cells [59], endothelial (HUVEC) cells [60], Calu 3 - cells [61], mouse retinal cells [62] or HCT-116 and MDA - MB-231 cancer cells [63]. It leads to the consideration of these complexes as non-cytotoxic or with low cytotoxic potential in the therapeutic range of dosage. However, the results of MTT assay solely indicate cell viability, without distinguishing between cytotoxic, cytostatic, or antiproliferative effects [64], thus complementary assays were conducted to aid in data analysis and interpretation alongside the MTT assay.

According to the presented results of alkaline comet assay, DMH, β-CD and their inclusion complexes prepared by kneading and solvent evaporation method did not show a genotoxic effect on PBMCs. The percentage of DNA in the comet tail did not significantly differ ($p > 0.05$) from negative control after treatment at a variety of concentrations. Treatments with inclusion complexes of DMH and β-CD prepared by solvent evaporation method at

concentrations of 36.36, 54.55, 72.73 and 90.91 ng mL^{-1} even exhibited significantly lower percentage of DNA in the comet tail compared to negative control ($p < 0.05$). For 5-FU, genotoxic effects were observed due to an increase in migration (mean tail length) of cell DNA compared to the untreated cells in negative control ($p < 0.05$). The mean value of tail intensity for the positive control was 61.6%, while, for the negative control it was 12.3 %. Mean % tail DNA values for all the treatments at various concentrations were from 6.7 to 14.5 respectively (Table 5). It implies that there were no significant increases in the induction of DNA strand breaks in the PBMCs at any dose compared to the negative control. DNA integrity of different inclusion complexes of β-CD and its hydrophilic derivate hydroxypropyl-β-CD (HP-β-CD) were examined by comet assay in cell line HL-60 [65], dermal fibroblasts of healthy subjects [66] or Niemann-Pick C1 patients [67], differentiated human macrophage-like THP1 cells [68], Jurkat cells (ATCC, clone E6-1) [69], human lymphocytes [70] and human leucocytes [71] and found to be safe, with no genotoxic effects shown. It is also reported that DMH did not cause DNA strand breaks in rat primary hepatocytes [72].

No significant differences were found in the CBMN cyt assay biomarkers analysis that would indicate genotoxic effects of all tested complexes. The frequencies of observed MNi, NBUDs and NPBs in all applied concentrations were not significantly increased compared to the negative control. It was even noticed that the frequency of total MNi as well as BN cells with MNi significantly decreased after treatment with complexes prepared by solvent evaporation method in all concentrations ($p < 0.005$) which definitely classifies this compound as non-genotoxic on normal PBMCs. Inclusion complexes of β-CD and its hydrophilic derivates (HP-β-CD, methyl-β-CD and sulfobutyl ether-β-CD) do not affect the frequency of genotoxicity biomarkers in human lymphocytes [73], THP1 cells [68] nor in Chinese hamster ovary-K1 cells [74]. The genotoxic effects of inclusion complexes β-CD were also evaluated *in vivo*, revealing no evidence of induced genetic damage [75,76]. As expected, a significant

increase of all biomarkers was found in the positive control. Cytotoxic and cytostatic potential was not determined for any of the tested complexes because no significance was found for the NDI and NDCI values between treatments and negative control. Considering the low cytotoxicity rate and high viability of PBMCs assessed by MTT assay, these results confirmed that the tested complexes do not have aneugenic or clastogenic effects in normal PBMCs. Although PBMCs offer numerous advantages regarding their accessibility and storage convenience [77], considering the absence of enzyme systems responsible for metabolic activation [78], observed cytotoxic and genotoxic effects could be perceived as relevant within the framework of this model. The advantage also lies in the use of primary PBMC culture regardless of the mentioned metabolic activation, which was not primarily necessary in this case.

The specificity of the genotoxicity assay may depend more on the particular test system used rather than the presence or absence of metabolic activation [79]. Gokarn et al. examined the cytotoxicity of DMH by MTT assay and metabolic activation was not performed [57]. Another study reported that DMH's metabolite, diphenhydramine, did not induce chromosomal abberations in cultured human lymphocytes or fibroblasts in the absence of exogenous metabolic activation [80].

PBMCs are used in genotoxicity testing and metabolic studies, but the use of metabolic activation with PBMCs depends on the specific research context, primarily on the research objectives and the compounds being tested.

The use of metabolic activation to simulate the metabolic processes that occur in the body and assess the genotoxic potential of compounds that require metabolic transformation to become genotoxic may not always be necessary with PBMCs, especially in studies focusing on the immediate metabolic response of PBMCs or assessing metabolic flexibility and capacity [81]. Therefore, PBMCs can be used both with and without metabolic activation in different research contexts, depending on the specific goals of the study and the need to

evaluate the genotoxic effects of compounds that require metabolic activation for their activity [82].

The limitation of the study is working on only one type of cell and solely on an *in vitro* model of primary human healthy cell culture (short-term), rather than on additional specific cell lines or some *in vivo* model. Additional research should involve a significantly larger number of *in vitro* cell models with preserved metabolic functions to validate these effects.

CONCLUSION

The analyses in this research indicate the formation of a new, stable inclusion complex between DMH and β-CD in a 1:1 stoichiometric ratio. Previously uninvestigated complex formation was confirmed by ATR-FTIR and DSC analyses according to the changes in ATR-FTIR spectra and the absence of characteristic endothermic peaks of DMH and β-CD in DSC thermograms of inclusion complexes. It was proved that both kneading and solvent evaporation methods successfully provided complexation.

Prior studies did not assess the cytotoxic and genotoxic potential of DMH-βCD inclusion complexes. Our findings from the MTT assay, comet assay, and CBMN cyt assay indicate no observed cytotoxic or genotoxic effects on normal PBMCs across five concentrations, two of which exceeded therapeutic levels. Given the absence of metabolic activation enzyme systems in lymphocytes, the observed cytotoxic and genotoxic effects might be relevant within this model, necessitating further research with more *in vitro* cell models to validate them.

Inclusion complexation with β-CD might be an efficient approach to overcome the poor solubility issues of DMH and to mask its bitter taste. It can be further investigated whether the newly formed, nontoxic complexes enhance the physicochemical properties of DMH in pharmaceutical formulations and if so, the DMH- β-CD system can be used in new drug delivery systems.

ACKNOWLEDGMENTS

REFERENCES

1. Maheswari DU, Anand T, Padma A, Ilaiyaraja N, Khanum F. Evaluation of the effect of herbal extracts and their bioactive compounds against motion sickness by regulating neurotransmitter levels in vitro and in vivo. South African J Bot 2020;130:130–40. https://doi.org/https://doi.org/10.1016/j.sajb.2019.12.012.

2. Leung AK, Hon KL. Motion sickness: an overview. Drugs Context 2019;8. https://doi.org/10.7573/dic.2019-9-4.

3. Abdul Rasool BK, Mohammed AA, Salem YY. The optimization of a dimenhydrinate transdermal patch formulation based on the quantitative analysis of in vitro release data by DDSolver through skin penetration studies. Sci Pharm 2021;89:1–22. https://doi.org/10.3390/scipharm89030033.

4. Jadhav YG, Galgatte UC, Chaudhari PD. Overcoming poor solubility of dimenhydrinate: Development, optimization and evaluation of fast dissolving oral film. Adv Pharm Bull 2018;8:721–5. https://doi.org/10.15171/apb.2018.081.

5. Khan Q, Shah SNH, Arshad MS, Usman F, Khalil R, Ul-Haq Z, et al. Formulation and optimization of dimenhydrinate emulgels for topical delivery using response surface methodology. Pak J Pharm Sci 2021;34:245–55. https://doi.org/10.36721/PJPS.2021.34.1.SUP.245-255.1.

6. Shah N, Dalvadi H, Naik P, Desai A, Patel N. Formulation and evaluation of immediate release tablet of cinnarizine and dimenhydrinate. Int J Pharma Sci Res 2016;7:185–9.

7. Jules-Léger, Inc. SC, Boucherville, QC CJ 7K8. Dimenhydrinate product monograph 2017:1–24. https://www.sandoz.ca/sites/www.sandoz.ca/files/Dimenhydrinate Product Monograph.pdf.

8. Boczar D, Michalska K. Cyclodextrin inclusion complexes with antibiotics and antibacterial agents as drug-delivery systems — A pharmaceutical perspective. Pharmaceutics 2022;14:1382. https://doi.org/https:// doi.org/10.3390/pharmaceutics 14071389.

9. Tang W, Zou C, Da C, Cao Y, Peng H. A review on the recent development of cyclodextrin-based materials used in oil fi eld applications. Carbohydr Polym 2020;240:116321. https://doi.org/10.1016/j.carbpol.2020.116321.

10. Jacob S, Nair AB. Cyclodextrin complexes: Perspective from drug delivery and formulation. Drug Dev Res 2018;79:201–17. https://doi.org/10.1002/ddr.21452.

11. Aslani A, Ghasemi A, Esfahani SK. Design, formulation and physicochemical evaluation of dimenhydrinate orally disintegrating tablets. Galen Med J 2018;7:936.

12. Szente L, Singhal A, Domokos A, Song B. Cyclodextrins: Assessing the impact of cavity size, occupancy, and substitutions on cytotoxicity and cholesterol homeostasis. Moleculeses 2018;23:1–15. https://doi.org/10.3390/molecules23051228.

13. Udrescu L, Sbârcea L, Fuliaș A, Ledeți I, Vlase G, Barvinschi P, et al. Physicochemical analysis and molecular modeling of the fosinopril β-cyclodextrin inclusion complex. J Spectrosc 2014;2014:748468. https://doi.org/10.1155/2014/748468.

27

14. Michel B, Heggset EB, Syverud K, Dufresne A, Bras J. Inclusion complex formation between sulfadiazine and various modified β-cyclodextrins and characterization of the complexes. J Drug Deliv Sci Technol 2022;76:103814. https://doi.org/https://doi.org/10.1016/j.jddst.2022.103814.

15. Jicsinszky L. Some comments on the cyclodextrin solubilities. MOJ Biorg Org Chem 2019;3:11–3. https://doi.org/10.15406/mojboc.2019.03.00091.

16. Shah PB, Goodyear BC, Michniak-Kohn B. A review : Enhancement of solubility and oral bioavailability of poorly soluble drugs. Adv Pharm J 2017;2:161–73.

17. Bhalani D V, Nutan B, Kumar A, Singh Chandel AK. Bioavailability enhancement techniques for poorly aqueous soluble drugs and therapeutics. Biomedicines 2022;10. https://doi.org/10.3390/biomedicines10092055.

18. Aiassa V, Garnero C, Longhi MR, Zoppi A. Cyclodextrin multicomponent complexes: Pharmaceutical applications. Pharmaceutics 2021;1099:1–26.

19. Tavares V, Macedo CC, Montanhez L, Barros FAP, Meurer EC, Campos DR, et al. Determination of dimenhydrinate in human plasma by liquid chromatography-electrospray tandem mass spectrometry: application to a relative bioavailability study. J Chromatogr B, Anal Technol Biomed Life Sci 2007;853:127–32. https://doi.org/10.1016/j.jchromb.2007.03.027.

20. Regenthal R, Krueger M, Koeppel C, Preiss R. Drug levels: therapeutic and toxic

serum/plasma concentrations of common drugs. J Clin Monit Comput 1999;15:529–44. https://doi.org/10.1023/a:1009935116877.

21. Higuchi, T; Connnors AK. Phase solubility techniques. Adv Anal Chem Instrum 1965;4:117–212.

22. Hindija L, Hadžiabdić J, Rahić O, Tucak-Smajić A, Sirbubalo M, Klebovich I, et al. Effect of molar mass of hydroxypropyl β-cyclodextrin on the aqueous solubility of dimenhydrinate. Acta Pharm Hungarica, Abstr DDRS 2021 Conf 2021;91:337–9. https://doi.org/10.33892/aph.2021.91.337-339.

23. de Melo NFS, Grillo R, Rosa AH, Fraceto LF. Interaction between nitroheterocyclic compounds with β-cyclodextrins: Phase solubility and HPLC studies. J Pharm Biomed Anal 2008;47:865–9. https://doi.org/https://doi.org/10.1016/j.jpba.2008.04.022.

24. Hindija L, Hadžiabdić J, Rahić O, Tucak-Smajić A, Šahinović M, Vranić E. Inclusion complexation with randomly methylated β-Cyclodextrin - An opportunity to achieve greater solubility of dimenhydrinate. In: Badnjević A, Gurbeta Pokvić L, editors. MEDICON'23 C., Cham: Springer Nature Switzerland; 2024, p. 383–91. https://doi.org/https://doi.org/10.1007/978-3-031-49062-0_42.

25. Histopaque -1077, Sigma Aldrich Product information n.d. chrome-extension://efaidnbmnnnibpcajpcglclefindmkaj/https://www.scientificlabs.co.uk/handlers/libraryFiles.ashx?filename=Technical_Data_Sheets_1_10771-100ML_A.pdf.

26. Bayoumi M, Arafa MG, Nasr M, Sammour OA. Nobiletin-loaded composite penetration

enhancer vesicles restore the normal miRNA expression and the chief defence antioxidant levels in skin cancer. Sci Rep 2021;11:20197. https://doi.org/10.1038/s41598-021-99756-1.

27. Li Y-Z, Zhang H-W, Fan H, Liang X-F, Song B, Chen H, et al. Steroidal constituents from Helleborus thibetanus and their cytotoxicities. Chin J Nat Med 2019;17:778–84. https://doi.org/10.1016/S1875-5364(19)30094-9.

28. Haverić A, Goletić Š, Durgut S, Hadžić M, Haverić S. Effects of curcumin and luteolin on viability and cell death induction in NFS-60 cell line. Genet Appl 2018;2:43–50. https://doi.org/10.31383/ga.vol2iss2pp43-50.

29. Suman G, Jamil K. Application of human lymphocytes for evaluating toxicity of anti-cancer drugs. Int J Pharmacol 2006;2:374–81. https://doi.org/10.3923/ijp.2006.374.381.

30. Ganguly K, Kulkarni AR, Aminabhavi TM. In vitro cytotoxicity and in vivo efficacy of 5-fluorouracil-loaded enteric-coated PEG-crosslinked chitosan microspheres in colorectal cancer therapy in rats. Drug Deliv 2015:1–14. https://doi.org/10.3109/10717544.2015.1089955.

31. Cetkovic T, Haveric A, Klacar LC, Omanovic MH. In vitro assessment of genotoxic and cytotoxic effects of Artemisia annua L . tincture. Genet Appl 2021;5:1–9. https://doi.org/10.31383/ga.vol5iss2pp1-9.

32. Lu Y, Liu Y, Yang C. Evaluating in vitro DNA damage using comet assay. J Vis Exp 2017. https://doi.org/10.3791/56450.

33. Costa S, Paulo Teixeira J. Comet Assay. In: Wexler P, editor. Encycl. Toxicol. (Third Ed. Third Edition, Oxford: Academic Press; 2014, p. 1020–3. https://doi.org/https://doi.org/10.1016/B978-0-12-386454-3.01072-1.

34. Møller P, Azqueta A, Boutet-Robinet E, Koppen G, Bonassi S, Milić M, et al. Minimum information for reporting on the comet assay (MIRCA): recommendations for describing comet assay procedures and results. Nat Protoc 2020;15:3817–26. https://doi.org/10.1038/s41596-020-0398-1.

35. Quintana-Sosa M, León-Mejía G, Luna-Carrascal J, De Moya YS, Rodríguez IL, Acosta-Hoyos A, et al. Cytokinesis-block micronucleus cytome (CBMN-CYT) assay biomarkers and telomere length analysis in relation to inorganic elements in individuals exposed to welding fumes. Ecotoxicol Environ Saf 2021;212:111935. https://doi.org/10.1016/j.ecoenv.2021.111935.

36. Fenech M. Cytokinesis-block micronucleus cytome assay. Nat Protoc 2007;2:1084–104. https://doi.org/10.1038/nprot.2007.77.

37. Fenech M, Chang WP, Kirsch-Volders M, Holland N, Bonassi S, Zeiger E. HUMN project: detailed description of the scoring criteria for the cytokinesis-block micronucleus assay using isolated human lymphocyte cultures. Mutat Res 2003;534:65–75. https://doi.org/10.1016/s1383-5718(02)00249-8.

38. Fenech M. The in vitro micronucleus technique. Mutat Res 2000;455:81–95. https://doi.org/10.1016/s0027-5107(00)00065-8.

39. Kondoros BA, Jójárt-Laczkovich O, Berkesi O, Szabó-Révész P, Csóka I, Ambrus R, et al. Development of solvent-free co-ground method to produce terbinafine hydrochloride cyclodextrin binary systems; Structural and in vitro characterizations. Pharmaceutics 2022;14. https://doi.org/10.3390/pharmaceutics14040744.

40. Cheirsilp B, Rakmai J. Inclusion complex formation of cyclodextrin with its guest and their applications. Biol Eng Med 2016;2:1–6. https://doi.org/10.15761/BEM.1000108.

41. Cid-Samamed A, Rakmai J, Mejuto JC, Simal-Gandara J, Astray G. Cyclodextrins inclusion complex: Preparation methods, analytical techniques and food industry applications. Food Chem 2022;384.

42. Patil JS, Kadam D V, Marapur SC, Kamalapur M V. Inclusion complex system: A novel technique to improve the solubility and bioavailability of poorly soluble drugs: A review. Int J Pharm Sci Rev Res 2010;2.

43. Preis M, Pein M, Breitkreutz J. Development of a taste-masked orodispersible film containing dimenhydrinate. Pharmaceutics 2012;4:551–62.

44. Preis M, Breitkreutz J. Development of orodispesible mini-patches for the treatment of vomiting and nausea. Eur Paediatr Formul Initiat 2011.

45. Faizatun F, Joenoes L, Nafisa S. Chewable tablet from inclusion complexes of dimenhydrinate-β-cyclodextrin using spray drying method. J Pharm Indones 2019;11:473–83.

46. Rao VM, Stella VJ. When can cyclodextrins be considered for solubilization purposes? J Pharm Sci 2003;92:927–32. https://doi.org/10.1002/jps.10341.

47. Ankit A, Kiran Kumar GB, Madhu BK. Formulation and evaluation of orodispersible tablets of dimenhydrinate by using co-processed superdisintegrants. J Sci Eng Technol 2016;12:23–33.

48. Abarca RL, Rodríguez FJ, Guarda A, Galotto MJ, Bruna JE. Characterization of beta-cyclodextrin inclusion complexes containing an essential oil component. Food Chem 2016;196:968–75. https://doi.org/10.1016/j.foodchem.2015.10.023.

49. Lin L, Dai Y, Cui H. Antibacterial poly(ethylene oxide) electrospun nanofibers containing cinnamon essential oil/beta-cyclodextrin proteoliposomes. Carbohydr Polym 2017;178:131–40. https://doi.org/https://doi.org/10.1016/j.carbpol.2017.09.043.

50. Venuti V, Stancanelli R, Acri G, Crupi V, Paladini G, Testagrossa B, et al. "Host-guest" interactions in Captisol®/Coumestrol inclusion complex: UV–vis, FTIR-ATR and Raman studies. J Mol Struct 2017;1146:512–21. https://doi.org/https://doi.org/10.1016/j.molstruc.2017.06.054.

51. Wang F, Yu W, Popescu C, Ibrahim AA, Yu D, Pearson R, et al. Cholecalciferol complexation with hydroxypropyl-β-cyclodextrin (HPBCD) and its molecular dynamics simulation. Pharm Dev Technol 2022;27:389–98. https://doi.org/10.1080/10837450.2022.2064492.

52. Ji-Sang K. Study of flavonoid/hydroxypropyl-β-cyclodextrin inclusion complexes by UV-VIS, FTIR, DSC and X-Ray diffraction analysis. Prev Nutr Food Sci 2020;25:449–56.

53. Putra OD, Yoshida T, Umeda D, Higashi K, Uekusa H, Yonemochi E. Crystal structure determination of dimenhydrinate after more than 60 years: Solving salt–cocrystal ambiguity via solid-state characterizations and solubility study. Cryst Growth Des 2016;16:5223–9. https://doi.org/10.1021/acs.cgd.6b00771.

54. Desai J, Alexander K, Riga A. Characterization of polymeric dispersions of dimenhydrinate in ethyl cellulose for controlled release. Int J Pharm 2006;308:115–23. https://doi.org/10.1016/j.ijpharm.2005.10.034.

55. Pralhad T, Rajendrakumar K. Study of freeze-dried quercetin-cyclodextrin binary systems by DSC, FT-IR, X-ray diffraction and SEM analysis. J Pharm Biomed Anal 2004;34:333–9. https://doi.org/10.1016/S0731-7085(03)00529-6.

56. Rodríguez-Tenreiro C, Alvarez-Lorenzo C, Concheiro Á, Torres-Labandeira JJ. Characterization of cyclodextrincarbopol interactions by DSC and FTIR. J Therm Anal Calorim 2004;77:403–11. https://doi.org/10.1023/B:JTAN.0000038981.30494.f4.

57. Gokarn K, Jadhav P, Sagar R, Pankar P, Odapalli S. Repurposing over-the-counter drugs and an iron-chelator as antibacterial agents. Biosci Biotechnol Asia 2022;19:1051–63.

58. Hasegawa T, Kondo Y, Koizumi Y, Sugiyama T, Takeda A, Ito S, et al. A highly sensitive probe detecting low pH area of HeLa cells based on rhodamine B modified beta-

cyclodextrins. Bioorg Med Chem 2009;17:6015–9. https://doi.org/10.1016/j.bmc.2009.06.046.

59. Tang P, Li S, Wang L, Yang H, Yan J, Li H. Inclusion complexes of chlorzoxazone with β- and hydroxypropyl-β-cyclodextrin: Characterization, dissolution, and cytotoxicity. Carbohydr Polym 2015;131:297–305. https://doi.org/10.1016/j.carbpol.2015.05.055.

60. Castagne D, Fillet M, Delattre L, Evrard B, Nusgens B, Piel G. Study of the cholesterol extraction capacity of β-cyclodextrin and its derivatives, relationships with their effects on endothelial cell viability and on membrane models. J Incl Phenom Macrocycl Chem 2009;63:225–31. https://doi.org/10.1007/s10847-008-9510-9.

61. Matilainen L, Toropainen T, Vihola H, Hirvonen J, Järvinen T, Jarho P, et al. In vitro toxicity and permeation of cyclodextrins in Calu-3 cells. J Control Release Off J Control Release Soc 2008;126:10–6. https://doi.org/10.1016/j.jconrel.2007.11.003.

62. Prajapati M, Christensen G, Paquet-durand F, Loftsson T. Cytotoxicity of β-cyclodextrins in retinal explants for intravitreal drug formulations. Molecules 2021;26:1–13.

63. Vukic MD, Vukovic NL, Popovic SL, Todorovic D V, Djurdjevic PM, Matic SD, et al. Effect of β-cyclodextrin encapsulation on cytotoxic activity of acetylshikonin against HCT-116 and MDA-MB-231 cancer cell lines. Saudi Pharm J SPJ Off Publ Saudi Pharm Soc 2020;28:136–46. https://doi.org/10.1016/j.jsps.2019.11.015.

64. Karakaş D, Ari F, Ulukaya E. The MTT viability assay yields strikingly false-positive viabilities although the cells are killed by some plant extracts. Turkish J Biol = Turk

Biyol Derg 2017;41:919–25. https://doi.org/10.3906/biy-1703-104.

65. Wilhelms B, Broscheit J, Shityakov S. Chemical analysis and molecular modelling of cyclodextrin-formulated propofol and its sodium salt to improve drug solubility, stability and pharmacokinetics (cytogenotoxicity). Pharmaceuticals 2023;16. https://doi.org/10.3390/ph16050667.

66. Donida B, Raabe M, Tauffner B, de Farias MA, Machado AZ, Timm F, et al. Nanoparticles containing β-cyclodextrin potentially useful for the treatment of Niemann-Pick C. J Inherit Metab Dis 2020;43:586–601. https://doi.org/https://doi.org/10.1002/jimd.12210.

67. Hammerschmidt TG, Donida B, Raabe M, Faverzani JL, de Fátima Lopes F, Machado AZ, et al. Evidence of redox imbalance and mitochondrial dysfunction in Niemann-Pick type C 1 patients: the in vitro effect of combined therapy with antioxidants and β-cyclodextrin nanoparticles. Metab Brain Dis 2023;38:507–18. https://doi.org/10.1007/s11011-022-01128-9.

68. Machelart A, Salzano G, Li X, Demars A, Debrie A-S, Menendez-Miranda M, et al. Intrinsic antibacterial activity of nanoparticles made of β-cyclodextrins potentiates their effect as drug nanocarriers against tuberculosis. ACS Nano 2019;13:3992–4007. https://doi.org/10.1021/acsnano.8b07902.

69. Diamantis DA, Ramesova S, Chatzigiannis CM, Degano I, Gerogianni PS, Karadima KE, et al. Exploring the oxidation and iron binding profile of a cyclodextrin encapsulated quercetin complex unveiled a controlled complex dissociation through a chemical

stimulus. Biochim Biophys Acta - Gen Subj 2018;1862:1913–24. https://doi.org/https://doi.org/10.1016/j.bbagen.2018.06.006.

70. Khan MJ, Ahmad A, Zamzami MA, Siddiqui S, Khan MA. Bidirectional approach of β-cyclodextrin-capped silver nanoparticles: reduction in toxicity and enhancement in antibacterial activity. Clean Technol Environ Policy 2023. https://doi.org/10.1007/s10098-023-02618-9.

71. Calabrò ML, Tommasini S, Donato P, Stancanelli R, Raneri D, Catania S, et al. The rutin/β-cyclodextrin interactions in fully aqueous solution: spectroscopic studies and biological assays. J Pharm Biomed Anal 2005;36:1019–27. https://doi.org/https://doi.org/10.1016/j.jpba.2004.09.018.

72. Brambilla G, Mattioli F, Robbiano L, Martelli A. Genotoxicity and carcinogenicity studies of antihistamines. Arch Toxicol 2011;85:1173–87. https://doi.org/10.1007/s00204-011-0659-4.

73. Hadžiabdić J, Kopjar N, Želježić D, Špirtović-Halilović S, Završnik D. Cytogenotoxicity of inclusion complexes of diazepam with 2-hydroxypropyl-β-cyclodextrin. Drug Res 2017;67:661–72. https://doi.org/10.1055/s-0043-115123.

74. Shah M, Shah V, Ghosh A, Zhang Z, Minko T. Molecular inclusion complexes of β-cyclodextrin derivatives enhance aqueous solubility and cellular internalization of paclitaxel: Preformulation and in vitro assessments. J Pharm Pharmacol 2015;2:8. https://doi.org/10.13188/2327-204X.1000011.

75. Halavach TM, Kurchenko VP, Tsygankow VG, Bondaruk AM, Tarun EI, Asafov VA. β-Cyclodextrin nanocomplexes with biologically active peptides from hydrolysed bovine whey and colostrum. Biointerface Res Appl Chem 2022;12:8502–14.

76. Zhang WF, Zhou HY, Chen XG, Tang SH, Zhang JJ. Biocompatibility study of theophylline/chitosan/β-cyclodextrin microspheres as pulmonary delivery carriers. J Mater Sci Mater Med 2009;20:1321–30. https://doi.org/10.1007/s10856-008-3680-2.

77. Wong L, Jiang K, Chen Y, Hennon T, Holmes L, Wallace CA, et al. Limits of peripheral blood mononuclear cells for gene expression-based biomarkers in juvenile idiopathic arthritis. Sci Rep 2016;6:29477. https://doi.org/10.1038/srep29477.

78. Pearce EL, Poffenberger MC, Chang C-H, Jones RG. Fueling immunity: insights into metabolism and lymphocyte function. Science 2013;342:1242454. https://doi.org/10.1126/science.1242454.

79. Tate MJ, Walmsley RM. The influence of exogenous metabolism on the specificity of in vitro mammalian genotoxicity tests. Mutagenesis 2017;32:491–9. https://doi.org/10.1093/mutage/gex017.

80. NTP toxicology and carcinogenesis studies of diphenhydramine hydrochloride (CAS No. 147-24-0) in F344/N Rats and B6C3F1 mice (feed studies). Natl Toxicol Program Tech Rep Ser 1989;355:1–176.

81. Janssen JJE, Lagerwaard B, Porbahaie M, Nieuwenhuizen AG, Savelkoul HFJ, van Neerven RJJ, et al. Extracellular flux analyses reveal differences in mitochondrial PBMC

metabolism between high-fit and low-fit females. Am J Physiol Endocrinol Metab 2022;322:141–53. https://doi.org/10.1152/ajpendo.00365.2021.

82. Debon E, Rogeboz P, Latado H, Morlock GE, Meyer D, Cottet-Fontannaz C, et al. Incorporation of metabolic activation in the HPTLC-SOS-Umu-C bioassay to detect low levels of genotoxic chemicals in food contact materials. Toxics 2022;10. https://doi.org/10.3390/toxics10090501.

83. Di Cagno MP. The potential of cyclodextrins as novel active pharmaceutical ingredients: A short overview. Molecules 2017;22. https://doi.org/10.3390/molecules22010001.

TABLES AND FIGURES WITH LEGENDS

TABLE 1. Solubility of DMH in aqueous solutions of various concentrations of β-CD at 25 °C ± 0.1 °C (n = 3)

S	S_{CD} (at 25ºC)	RSD	S_{CD}/S_o
4.40	17.35	0.71	0.86
7.49	19.12	0.87	0.95
8.81	19.93	0.40	0.98
10.57	21.42	1.24	1.06
13.21	22.85	1.81	1.13
15.86	25.27	0.60	1.25
17.62	26.68	0.96	1.32
22.03	31.15	0.91	1.55

S: Concentration of β-CD; S_{CD}: Concentration of DMH in CD solution (mmol L^{-1}); RSD: Relative standard deviation; S_{CD}/S_o: Solubility enhancement factor calculated as the ratio of drug solubility in CD solution (S_{CD}) versus drug solubility value (S_o) measured in the absence of CD.

TABLE 2. Essential parameters for complexation of DMH and β-CD determined by phase solubility analysis

Slope[e]	R^{2e}	K_s $(M^{-1})^f$	CE^g	Dose[h] (mg)	D : CD[i]	U_{CD}^j
0.7751	0.9881	171.10	3.45	25	1 : 1.29	0.214

[e]Values obtained directly from the drug phase solubility diagram; [f] The K_s calculated from the slope of phase solubility diagram according to Equation (1); [g]Complexation efficiency calculated from the slope of phase solubility diagram according to Equation (2); [h]Oral dosage of DMH for children; [i]The drug: cyclodextrin molar ratio is based on the calculated complexation efficiency according to Equation (3); [j]The utility number was calculated according to Equation (4). The U_{CD} was calculated for the values of K_s, S_o for DMH determined at 25 °C. The presented results for the U_{CD} are related to the working concentration of 1% CD.

TABLE 3. Comparison between the intensity of FTIR signals of pure DMH and binary systems with β-CD (physical mixture, inclusion complex prepared by kneading method and inclusion complex prepared by solvent evaporation method)

Parameter	Sample	Functional group			
		ν[-NH$_2$ and -NH]	ν[C=O]	ν[C=C aromatic]	ν[C-Cl carbonyl]
Wavenumber (cm^{-1})	DMH	3059.6	1644.3	1112.9	749.3
	P. M.	overlapped	1645.6	1114.1	751.1
	Dβ-K	overlapped	1689.0	1074.2	751.1
	Dβ-SE	overlapped	1682.7	1067.5	698.9
Changes |Δδ|	P. M.	/	1.3	1.2	1.8
	Dβ-K	/	44.7	38.7	1.8
	Dβ-SE	/	38.4	45.4	50.4
Transmittance (%)	DMH	76.95	26.79	31.27	30.17
	P. M.	n. o.[*]	45.36	67.20	47.90
	Dβ-K	n. o.[*]	82.41	56.72	53.74
	Dβ-SE	n. o.[*]	76.13	68.36	57.60

$|\Delta\delta| = \delta_{(binary\ sistem)} - \delta_{(pure\ DMH)}$; P.M. is abbreviation for physical mixture. Dβ-K is abbreviation for inclusion complex of DMH and β-CD prepared by kneading method. Dβ-SE is abbreviation for inclusion complex of DMH and β-CD prepared by solvent evaporation method. [*]peak of the functional group was not observed in binary system and % of transmittance could not be read.

TABLE 4. Comparison between the intensity of FTIR signals of pure β-CD and binary systems with DMH (physical mixture, inclusion complex prepared by kneading method and inclusion complex prepared by solvent evaporation method)

Parameter	Sample	Functional group			
		ν[OH]	ν[-CH$_2$ and -CH]	ν[H-O-H]	ν[C-O-C]
Wavenumber (cm^{-1})	**β-CD**	3317.3	2926.0	1645.6	1019.4
	P. M.	3311.7	2926.0	1640.8	1019.4
	Dβ-K	3289.4	2920.4	1648.8	1025.0
	Dβ-SE	3277.8	2919.8	1621.9	1023.4
Changes |Δδ|	**P. M.**	5.6	0	4.8	0
	Dβ-K	27.9	5.6	39.5	5.6
	Dβ-SE	39.5	6.2	23.7	4.9
Transmittance (%)	**β-CD**	64.97	77.86	88.69	35.18
	P. M.	62.42	76.86	68.60	21.39
	Dβ-K	59.97	74.50	57.41	29.57
	Dβ-SE	58.94	72.79	69.04	35.06

$|\Delta\delta| = \delta_{(binary\ sistem)} - \delta_{(pure\ \beta\text{-}CD)}$; P.M. is abbreviation for physical mixture. Dβ-K is abbreviation for inclusion complex of DMH and β-CD prepared by kneading method. Dβ-SE is abbreviation for inclusion complex of DMH and β-CD prepared by solvent evaporation method; peak of the functional group was not observed in binary system and % of transmittance could not be read

TABLE 5. Tail intensity (%) in PBMCs exposed to different concentrations of the tested treatments (mean ± SD)

Concentration of DMH (ng mL^{-1})	Pure DMH	Inclusion complex kneading method	Inclusion complex solvent evaporation method
36.36	2.51 ± 1.77	3.10 ± 1.28	1.79 ± 2.21
54.55	2.83 ± 1.54	3.04 ± 1.28	1.92 ± 2.23
72.73	3.44 ± 1.13	2.95 ± 1.43	2.53 ± 1.72
90.91	3.47 ± 1.08	2.88 ± 1.63	2.75 ± 1.27
109.9	3.59 ± 0.79	2.79 ± 1.55	3.57 ± 0.99
Concentration of β-CD (ng mL^{-1})	Pure β-CD	Negative control	Positive control 5-FU (100 μg mL^{-1})
250	3.02 ± 1.45	3.22 ± 1.21	5.93 ± 0.23
500	3.22 ± 1.09	/	/
750	3.25 ± 1.02	/	/
1000	3.42 ± 1.08	/	/

TABLE 6. Representative comet images from treatment of PBMCs with pure DMH, pure β-CD and their inclusion complexes prepared by kneading and solvent evaporation method

Negative control	
Positive control	
DMH	
β-CD	
Inclusion complex - kneading method	
Inclusion complex - solvent evaporation method	

TABLE 7. Results of CBMN cyt biomarkers frequency and NDI and NDCI values in treatments with pure DMH, inclusion complexes prepared by kneading method (Dβ-K) and solvent evaporation method (Dβ-SE)) (mean ± SD)

Treatments[t]	Total MNi	BN cells with MNi	NBUDs	NPBs	NDI	NDCI
Negative control	7.5 ± 2.38	7.25 ± 2.41	0.75 ± 0.5[s]	0.5 ± 0.58	1.576 ± 0.10	1.569 ± 0.10
DMH 1	4.25 ± 0.96[r, s]	4 ± 1.25[a]	0.75 ± 0.96[s]	0.25 ± 0.5	1.605 ± 0.10	1.600 ± 0.09
DMH 2	6.5 ± 1.92[s]	5.75 ± 1.92	1.75 ± 1.26[s]	0.25 ± 0.5	1.728 ± 0.10	1.718 ± 0.10
DMH 3	6.5 ± 2.38[s]	6.5 ± 2.34	1 ± 0.82[s]	0.25 ± 0.5	1.674 ± 0.12	1.667 ± 0.12
Dβ-K 1	6.25 ± 2.22[s]	6 ± 2.18	1.75 ± 0.5[s]	0.25 ± 0.5	1.704 ± 0.10	1.699 ± 0.11
Dβ-K 2	9 ± 4.08[s]	8.5 ± 3.45	0.75 ± 0.96[s]	0.5 ± 0.58	1.770 ± 0.06	1.759 ± 0.06
Dβ-K 3	8.25 ± 3.20[s]	8.25 ± 3.06	0.75 ± 0.5[s]	0.5 ± 0.58	1.775 ± 0.13	1.768 ± 0.13
Dβ-SE 1	2.75 ± 2.63[r, s]	2.75 ± 2.15[r]	1.25 ± 0.96[s]	0	1.617 ± 0.08	1.613 ± 0.08
Dβ-SE 2	3.5 ± 0.58[r, s]	3.5 ± 1.04[r]	0.25 ± 0.5[s]	0.25 ± 0.5	1.635 ± 0.19	1.628 ± 0.19
Dβ-SE 3	3.5 ± 2.08[r, s]	3.25 ± 1.61[r]	1.25 ± 1.5[s]	0.25 ± 0.5	1.570 ± 0.17	1.564 ± 0.17
Positive control	19.25 ± 6.65	19 ± 6.56	3.5 ± 1.92	1 ± 0.82	1.612 ± 0.01	1.577 ± 0.01

[r]significant decrease ($p < 0.005$) compared to negative control; [s]significant decrease ($p < 0.005$) compared to positive control; [t]concentration [ng mL^{-1}] of pure DMH and DMH in complexes were 1 (72.73), 2 (90.91) and 3 (109.09).
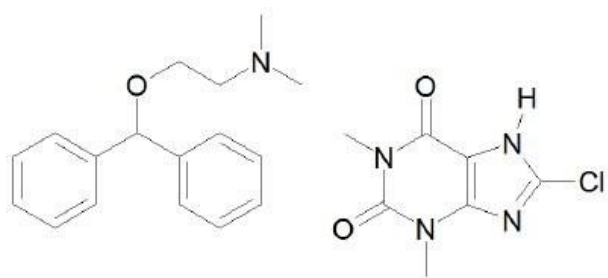
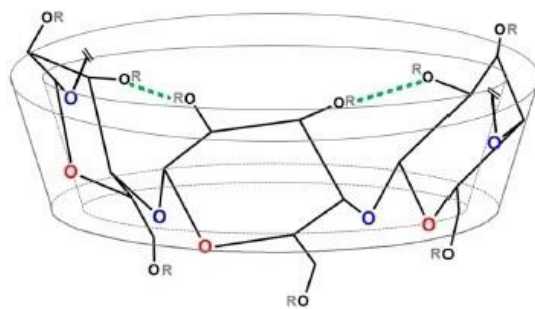**FIGURE 1. Chemical structure of dimenhydrinate (diphenhydramine, left and 8-chlorotheophylline, right) [43].**

FIGURE 2. Structure of β-cyclodextrin molecule. Green lines represent intramolecular hydrogen bonds that are formed when there are no hydrophilic substituents [83].
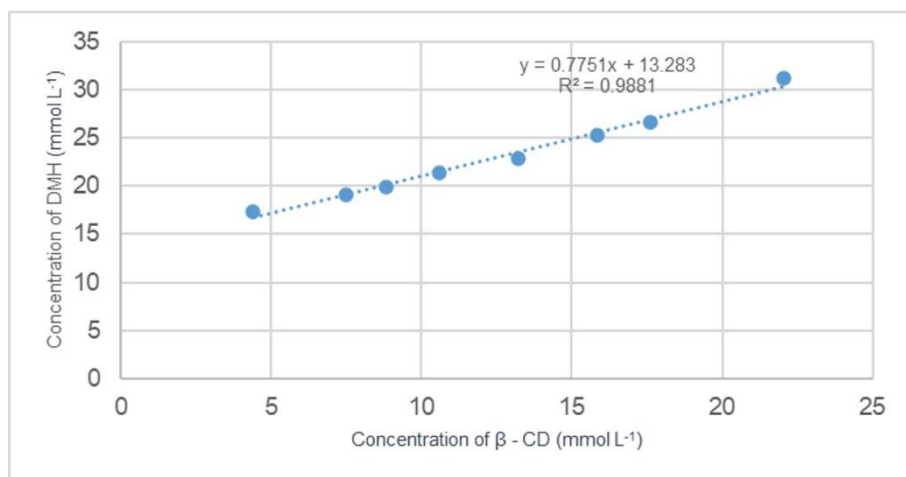
FIGURE 3. Phase solubility diagram of DMH in aqueous solution of β-CD.

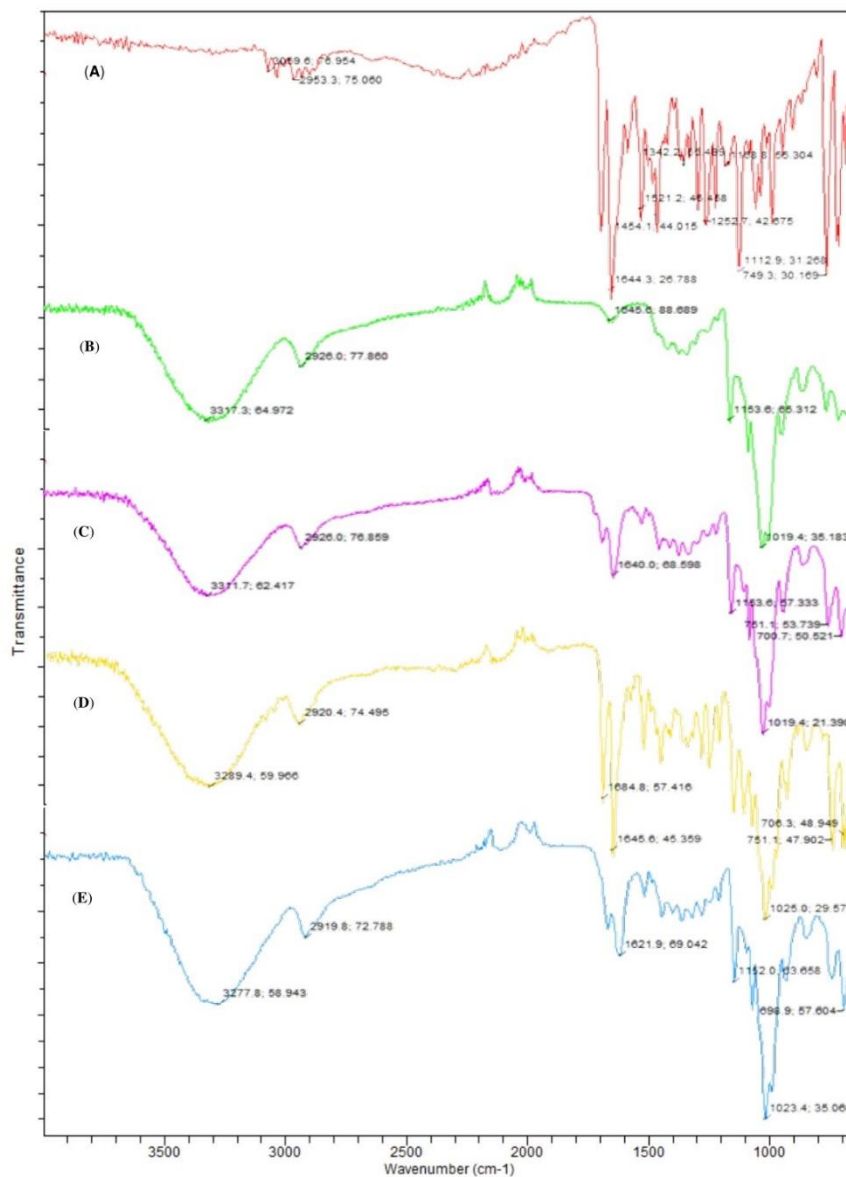**FIGURE 4. FTIR spectra of pure DMH (A), pure β-CD (B), their physical mixture (C), inclusion complex of DMH and β-CD prepared by kneading method (D) and inclusion complex of DMH and β-CD prepared by solvent evaporation method.**
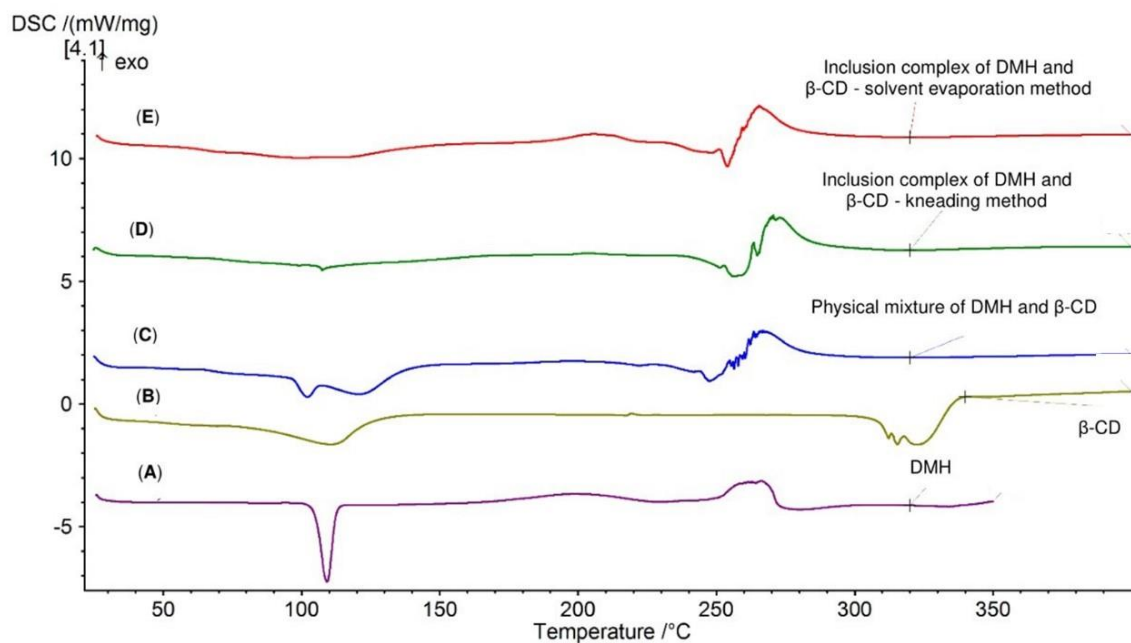
FIGURE 5. DSC thermograms of pure DMH (A), pure β-CD (B), their physical mixture (C), inclusion complex of DMH and β-CD prepared by kneading method (D) and inclusion complex of DMH and β-CD prepared by solvent evaporation method (E).
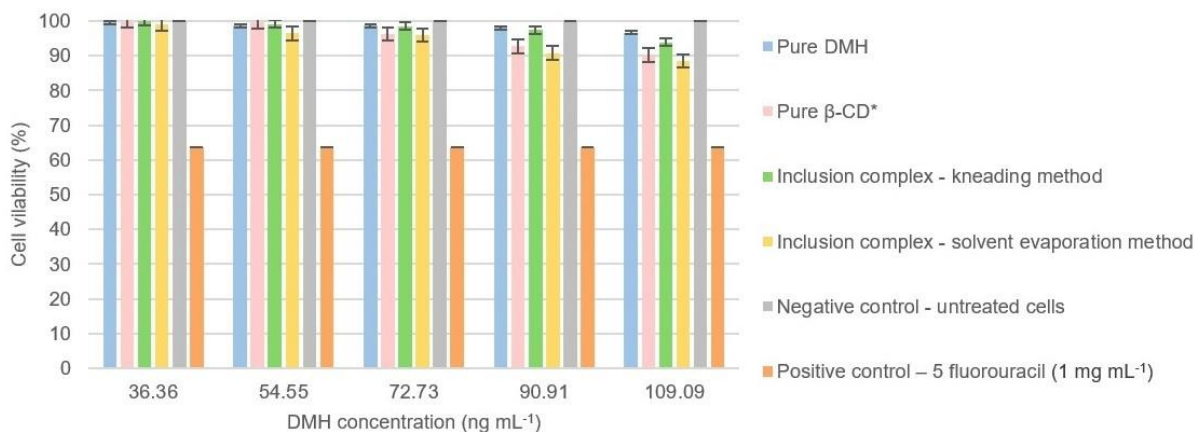
FIGURE 6. Percentage of cell viability in human PBMCs after treatment with pure DMH, pure β-CD and their inclusion complexes prepared by kneading and solvent evaporation method. *Pure β-CD was applied in concentration of 0, 250, 500, 750 and 1000 ng mL^{-1}.